SAVer: Structure-Aware Validation of Standard Fetal Head Planes via Clinically Grounded Anatomical Completeness

Anusha A[1], Vasanth Ambrose[1], Padmini Ramesh[2], Shyam Ayyasamy[2], Keerthi Ram[4], Suresh Seshadri[3], Manojkumar Lakshmanan[2], and Mohanasankar Sivaprakasam[1]

[1] Department of Electrical Engineering, Indian Institute of Technology, Madras (IITM), India
[2] Healthcare Technology Innovation Centre (HTIC),IITM, India
[3] Mediscan Systems, Chennai, India
[4] Sudha Gopalakrishnan Brain Centre,IITM, India
anusha@htic.iitm.ac.in, mohan@ee.iitm.ac.in

Abstract. Standard fetal head plane identification in ultrasound is essential for accurate biometric measurements and early detection of neuro developmental abnormalities. Automating the identification of these planes can optimize diagnostic workflows. Existing approaches predominantly treat plane identification as a global image-level classification task, often relying on superficial visual features rather than clinically defined anatomical criteria. To address these limitations, we propose **SAVer**, structure-aware validation framework that couples anatomical reasoning with plane classification to ensure clinically consistent fetal ultrasound plane identification. SAVer integrates anatomical segmentation with plane identification through a unified architecture that combines a perception backbone with a Plane Classification Module along with an Anatomical Reasoning Engine. The reasoning module explicitly evaluates the presence, completeness, and structural consistency of clinically relevant landmarks to ensure alignment with diagnostic standards. In addition, we introduce a Adapter Feature Alignment Module (AFAM) that enables efficient feature alignment between anatomical segmentation representations and plane classification.We evaluate the proposed method on fetal ultrasound head plane data, achieving a structure-size weighted dice score of 95% for anatomical segmentation and demonstrating improved robustness. The proposed structure-aware framework enhances interpretability and reliability by embedding clinically meaningful constraints into the classification process.

Keywords: Fetal Brain Ultrasound · Standard Plane Identification · Structure Aware Learning · Anatomical Segmentation.

1 Introduction

Fetal Ultrasound is the most widely used modality for antenatal screening due to its safety and clinical accessibility. Precise acquisition of fetal standard head planes specifically Transventricular (TV), Transthalamic (TT) and Transcerebellar (TC) planes[14] are crucial for biometric measurements[5][1][2] and detection of neuro developmental anomalies[18]. Automating the identification of these planes can significantly optimize diagnostic workflows. However, reliable plane recognition remains challenging due to variability in fetal pose, probe orientation, and inter-operator acquisition differences, which frequently result in incomplete or ambiguous visualization of critical anatomical structures.

Existing methods for plane classification approaches this as an image level task by utilizing Convolutional Neural Networks (CNN)[4] and transformer[15][9] based architectures to learn discriminative representations in a latent feature space. In these frameworks, the structural information is progressively compressed into a low-dimensional global embedding from which the final prediction is derived. The abstract appearance statistics are encoded rather than explicitly modeling anatomically meaningful structures. Consequently, predictions are driven by learned correlations in feature space rather than verification of clinically required structural criteria. In contrast, anatomical structure segmentation operates directly in the input (pixel) space, producing spatially grounded masks corresponding to specific structures. A clinically valid standard plane is characterized by the presence, geometry and spatial relationships of multiple inner structures[14], for instance, the presence of Cerebellum and Cavum Septum Pellucidi (CSP) simultaneously represents the TC plane. Despite advances in anatomical structure segmentation for fetal ultrasound[16],[12],[8], segmentation is often treated as an independent task, with limited integration into standard plane classification frameworks. This separation between feature-level classification and pixel-level anatomical reasoning restricts interpretability and clinical reliability.Without explicit anatomical supervision, classification may be driven by global head morphology rather than the landmarks defining a standard plane.[19]. Consequently, there remains a critical need for frameworks that explicitly encode anatomical structure presence[13] into the plane classification process. To address the above limitations we propose structure-aware framework for fetal brain plane classification. Our contributions are four fold:

- **Comprehensive Multi Structure Segmentation:** We segment 32 clinically relevant inner fetal brain structures, which, to the best of our knowledge, represents the most comprehensive anatomical delineation for supporting downstream tasks such as biometric assessment, structural consistency analysis and anomaly identification.
- **Integrated SAVer Framework:** We develop a unified anatomy driven framework that leverages both global image features and localized anatomical structures to ensure classification aligns with clinical diagnostic criteria.
- **Anatomical Reasoning Engine:** We implement a reasoning module that explicitly evaluates the presence, visibility, and spatial relationships of key anatomical landmarks, providing a "ultrasonographer-in-the-loop" logic to the automated classification process.
- **Adapter based feature alignment module:** We introduce a lightweight adapter module that enables efficient task-specific feature alignment without

requiring full encoder retraining, preserving the generalization capability of the foundation model.

2 Dataset and Methodology

Dataset: We curated a dataset retrospectively from a tertiary clinical center, consisting of 400 TC, 325 TT, and 370 TV fetal ultrasound images, totaling 1,095 samples. Each image was annotated by two clinical experts and verified by two independent reviewers, covering 32 unique anatomical structures across all planes. As anatomical requirements are plane-specific, each plane includes a defined subset of structures according to clinical guidelines.

Architecture: The proposed SAVer framework, as shown in Fig. 1, processes an ultrasound(US) image I $\in \mathbb{R}^{3\times H\times W}$ as input and predicts whether it satisfies the criteria for a standard fetal head plane. Let $c \in \{TT, TC, TV\}$ denote the plane labels where C denotes the number of planes. This estimates $Y \in \{0,1\}^{K\times H\times W}$ segmentation masks where K represents the number of anatomical structures. The US image is processed by a fine-tuned MedSAM ViT-B[6][11] encoder ξ to extract hierarchical feature representations as shown in Eq.1

$$f_{us} = \xi(I), \quad where \quad f_{us} \in \mathbb{R}^{256\times H\times W} \tag{1}$$

To enhance discriminative anatomical responses, the encoder features are refined using the Convolution Block Attention Module (CBAM)[17] which sequentially performs channel and spatial alignment to obtain f'_{us}. The refined features are processed by a lightweight decoder and segmentation heads to generate logits, which are then used to produce segmentation maps $\hat{Y}_k$ for localizing key anatomical structures in Eq.2

$$\hat{\mathbf{Y}}_k = \mathcal{H}_k\left(f_{us'}\right), \quad \hat{\mathbf{Y}}_k \in \mathbb{R}^{H\times W}, \quad k = 1, 2, \ldots, 32. \tag{2}$$

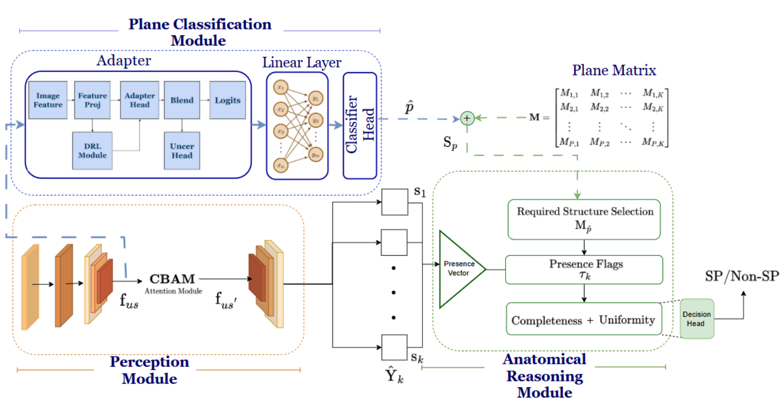

Fig. 1: SAVer framework: MedSAM-based multi-structure segmentation and adapter-based plane classification integrated with plane-aware anatomical reasoning for standard-plane validation.

While anatomical structures are localized in a bottom-up manner, structural validity is inherently plane-dependent. Different standard planes require distinct subsets of anatomical landmarks. Therefore, explicit plane prediction is necessary to provide contextual conditioning for structural reasoning. Thus, the encoder features f_{us} are then passed on to Global Average Pooling(GAP) module to obtain a pooled embedding feature vector $f_c \in \mathbb{R}^{256}$. The pooled embedding is projected into a higher dimensional latent space as depicted in Eq 3 to align with the transformer embedding dimensionality.

$$z = W_p f_c + b_p, \quad W_p \in \mathbb{R}^{768\times256}, z \in \mathbb{R}^{768} \tag{3}$$

The projected feature is passed through a bottleneck adapter [7], where the DRL module, uncertainty head, and blend operation enable lightweight task-specific adaptation, yielding a DRL-enhanced feature z_d, uncertainty estimate u, and adapted feature z_a:

$$z_a = \mathrm{Blend}(z + W_u\sigma(W_d z_d), u)\,, \quad z_d = \mathcal{H}_{DRL}(z),\ u = \mathcal{H}_{unc}(z_d), \tag{4}$$

The plane logits are then computed using a linear classifier head as in Eq. 5

$$\hat{p} = Softmax(W_c z_a + b_c), \quad \hat{p} \in \mathbb{R}^C \tag{5}$$

To explicitly model anatomical validity, we define a clinician-curated plane structure dependency matrix$M \in \{0,1\}^{C\times K}$, where $M_{c,k} = 1$ indicates that the structure k is required for the plane C. Anatomical evidence for the presence of a structure can be obtained from the predicted segmentation maps $\hat{Y_k}$, from which we compute a continuous structural presence score as denoted in Eq. 6

$$s_k = \frac{1}{HW}\sum_{i=1}^{H}\sum_{j=1}^{W}\hat{\mathbf{Y}}_k(i,j), \quad \mathbf{s} \in \mathbb{R}^K. \tag{6}$$

Here, s_k quantifies the normalized spatial extent of the K^{th} structure serving as a soft estimate of the anatomical presence. Given the predicted plane probabilities $\hat{p}$, the expected structure requirement vector that softly encodes which anatomical structures are expected under the predicted plane is given by Eq. 7

$$\mathbf{m} = \hat{p}^T M, \quad \mathbf{m} \in [0,1]^K \tag{7}$$

During training, we introduce a plane-aware anatomical loss that enforces minimum structural presence similar to [3] for extremely crucial anatomical landmarks.The required minimum structural presence is defined as shown in Eq. 8

$$\theta_k = \tau_k + \Delta_k, \tag{8}$$

where τ_k denotes the predefined minimal anatomical threshold and Δ_k is a learnable margin parameter.The resulting plane-aware anatomical loss in Eq.10, together with the segmentation and classification terms, forms the overall training objective defined in Eq. 10.

$$\mathcal{L}_{seg} = \mathcal{L}_{Dice} + \mathcal{L}_{Focal} + \mathcal{L}_{SoftHD} + \mathcal{L}_{L2}, \qquad \mathcal{L}_{cls} = \mathcal{L}_{CCE} \tag{9}$$

$$\mathcal{L} = \mathcal{L}_{seg} + \lambda_{cls}\mathcal{L}_{cls} + \lambda_{anatomy}\left[\sum_{k=1}^{K} m_k\,\mathrm{Softplus}(\theta_k - s_k)\right] \tag{10}$$

Plane-Aware Structured Confidence Aggregation: Let $p_{\max} = \max(\hat{p})$ denote the predicted plane confidence. In addition, five complementary anatomical quality measures are derived from the segmentation maps: c_{struct}, the mean pixel-wise segmentation confidence within detected structures; c_{comp}, a completeness score that verifies the presence and sufficient extent of plane-specific mandatory anatomy; c_{uni}, the coefficient of variation of structure areas measuring anatomical balance; c_{dist}, a spatial plausibility score based on the distribution of structures across image quadrants; and c_{edge}, a framing quality score that penalizes structures intersecting image boundaries. Together, these metrics assess prediction certainty, anatomical completeness, balance, spatial consistency, and acquisition quality. All measures are normalized to $[0, 1]$ and aggregated into a unified structured confidence score defined in Eq. 11.

$$C_{std} = w_1 p_{\max} + w_2 c_{struct} + w_3 c_{comp} + w_4 c_{uni} + w_5 c_{dist} + w_6 c_{edge}, \tag{11}$$

where $\sum_{i=1}^{6} w_i = 1$. The final plane validity prediction is obtained by thresholding the aggregated confidence as defined in Eq. 12,

$$\hat{y}_{valid} = \mathbb{1}(C_{std} \geq \delta)\,, \tag{12}$$

where δ is a predefined decision threshold.

3 Results and Discussion

Implementation Details: The model was trained on 1,095 TC, TT, and TV fetal US images, with 240 images (89 TC, 91 TT, and 60 TV) used for validation and testing.The model was trained for 60 epochs using the AdamW[10]optimizer with an initial learning rate of 10^{-4} freezing the encoder for the first 30 epochs before joint fine-tuning. All experiments were conducted on NVIDIA RTX 4090 GPU achieving an average inference time of 0.44 s per image. Fig.2A depicts the predicted segmentations of inner key structures along with input images of the fetal head planes like TV,TC and TT. Fig. 2B shows the radar plot for the weighted confidence along with overall SAVer score

Standard Plane Validity Assessment: The proposed SAVer framework was evaluated for standard plane validity discrimination on a test cohort of 240 fetal brain ultrasound frames containing both standard and non-standard acquisitions as shown in Tab.1. Performance was assessed using Accuracy, Precision, Recall, F1-score, and False Negative Rate (FNR), with emphasis on minimizing missed valid planes. Across all three planes, the model achieves high classification performance with F1-scores exceeding 91, indicating reliable discrimination between protocol-compliant and non-compliant frames. Notably, the FNR remains consistently low (≤ 0.05), demonstrating that valid diagnostic planes are rarely rejected.While the False Positive Rate (FPR) ranges from 0.20 to 0.36, SAVer demonstrates high sensitivity for standard plane detection, helping preserve diagnostically useful frames. At the same time, specificity remains critical

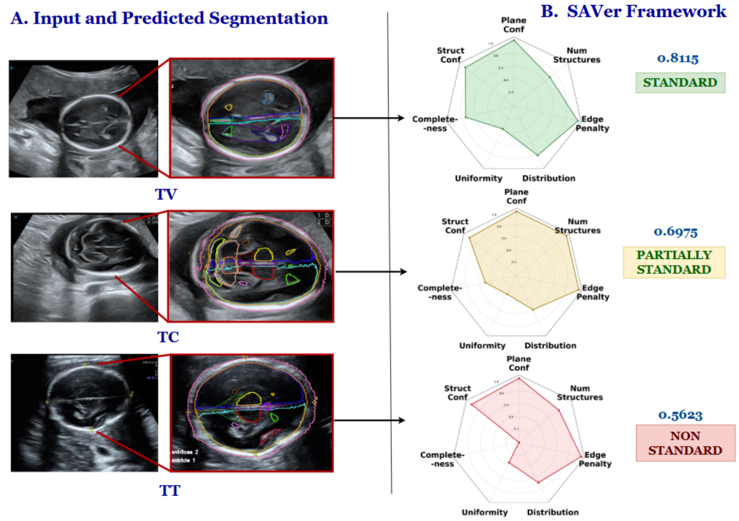

Fig. 2: SAVer framework (A) Input fetal ultrasound images and corresponding predicted multi-structure segmentations. (B) Radar-based confidence analysis for standard plane validity.

for reliable biometry estimation, and future improvements will focus on further reducing false positives while maintaining strong detection performance.

Table 1: Standard Plane Classification Performance

Plane	**Accuracy**(%)↑	**Recall**(%)↑	**Precision**(%)↑	**F1 Score**(%)↑	**FPR**↓	**FNR**↓
TC	88.16	96.10	85.00	91.89	0.36	0.02
TT	88.57	94.44	91.07	92.73	0.31	0.05
TV	95.12	96.36	98.15	97.25	0.20	0.03

Anatomical Localisation and Structural Integrity: We evaluate anatomical segmentation performance across the three standard fetal brain planes for 32 key structures using Dice, area-weighted Dice, IoU, and HD95 as shown in Tab.2. SAVer achieves macro Dice scores ranging from 68.76% to 72.58%, with the highest performance on the TV plane. The 32 structures vary considerably in size, from large regions to small fine-grained anatomies, and the lower macro Dice is mainly due to the inclusion of these smaller, inherently challenging structures as seen in Fig. 3.In contrast, area-weighted Dice consistently exceeds 95% across all planes, demonstrating robust performance on clinically dominant structures and effective mitigation of class imbalance. IoU values remain stable, indicating consistent regional overlap despite anatomical variability, while HD95 distances are confined to 17–18 pixels, reflecting stable boundary delineation with limited extreme contour deviations. Overall, this strong segmentation consistency supports the model's anatomical reasoning for standard plane validation, as accurate localization of required structures enables reliable completeness and presence verification.

Table 2: Anatomical Segmentation Performance

Plane	**Dice**(%)↑	**Weighted Dice**(%)↑	**IOU**↑	**HD95**(px)↓
TC	68.76	95.44	58.01	18.25
TT	69.67	95.52	58.88	17.39
TV	72.58	96.81	63.86	18.25

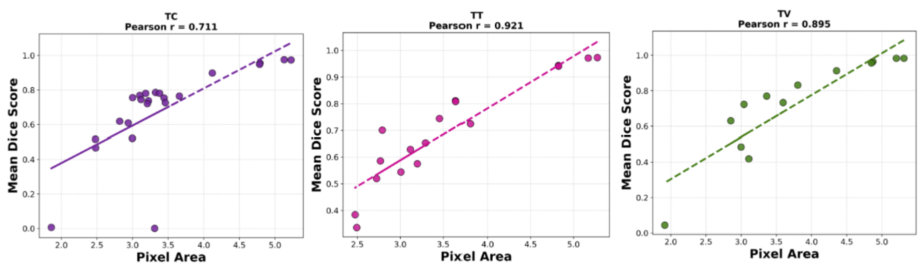

Fig. 3: Size–accuracy correlation across planes.Mean Dice score increases with anatomical structure size for TC, TT, and TV planes, with strong positive correlations.

Clinical Reliability Analysis On the validation set of TV plane consisting of 60 US images, the model achieved 95% accuracy and 96.4% sensitivity for standard-plane detection, with a low unsafe acceptance rate of 1.7% false positives. Confidence analysis showed clear separation between correct and incorrect predictions, with misclassifications concentrated at lower confidence levels, indicating reliable uncertainty estimation. The risk–coverage curve further demonstrated that most errors occur in low-confidence cases; restricting acceptance to the top 80% most confident predictions increased accuracy to 97.9% as can be seen in Fig.4. These results highlight high sensitivity, low clinical risk, and effective uncertainty awareness, supporting the model's use as a safety-oriented, real-time quality assurance tool for fetal neurosonography.

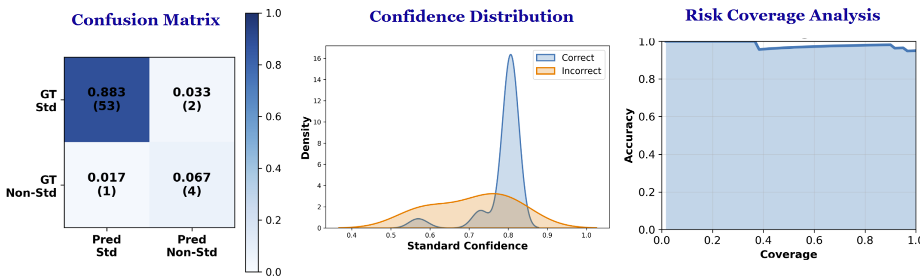

Fig. 4: Clinical Risk and Uncertainty Analysis. Confusion matrix (left) shows low unsafe acceptance. Confidence distributions (middle) separate correct and incorrect predictions, and the risk–coverage curve (right) demonstrates improved accuracy when low-confidence cases are deferred.

Ablation Study We conducted a systematic ablation study to quantify the utility of each architectural component as shown in Tab 3. The baseline only classification model though gives an accuracy of 72.80%, is repressed by high FPR and FNR of 0.52 and 0.31 respectively. This implies that this would lead to false classification of non diagnostic planes. The integration of segmentation and the structure presence vector increased the performance improving the metrics while reducing the FNR upto 0.06. While addition of uniformity slightly reduces the accuracy, it also reduced the FNR to 0.02.The complete SAVer framework attained a peak accuracy of 90.61% and an F1-score of 93.95%. Clinically, this high precision (91.40%) ensures that captured images adhere to anatomical standards, while the concurrent minimization of FPR (0.29) and FNR (0.03) significantly reduces the cognitive load on sonographers and mitigates operator-dependent variability.

Table 3: Ablation study evaluating the contribution of each architectural component to standard-plane detection performance.

Model Variant	**Accuracy**(%)↑	**Recall**(%)↑	**Precision**(%)↑	**F1 Score**(%)↑	**FPR**↓	**FNR**↓
Only CLS	72.80	68.50	75.20	71.70	0.52	0.31
CLS + Seg	77.72	73.95	88.24	81.96	0.30	0.41
CLS + Seg + Struct	82.01	94.38	79.97	88.24	0.32	0.06
CLS + Seg + Struct + Uni	79.91	92.21	77.43	89.23	0.48	0.02
SAVer (Full Model)	**90.61**	**95.68**	**91.40**	**93.95**	**0.29**	**0.03**

4 Conclusion and Future Works

The SAVer framework improves automated ultrasound quality assurance by combining anatomical segmentation with structure-aware reasoning. The ablation study demonstrates the importance of this multi-task design, achieving a peak accuracy of 90.61% and an F1-score of 93.95%. By explicitly verifying the presence and spatial arrangement of clinically relevant anatomical structures, SAVer provides an objective mechanism for standard-plane quality assessment that can support sonographers during image acquisition and reduce variability in plane selection. From a clinical perspective, such automated quality control has the potential to improve workflow efficiency, standardize image acquisition, and provide immediate feedback during fetal ultrasound examinations. Future work will focus on prospective multi-center validation across diverse scanners, operators, and patient populations to establish robustness in real-world settings. We also plan to extend the framework beyond binary standard/non-standard assessment to support graded plane quality evaluation, integrate anomaly-aware analysis of anatomical structures, and optimize the system for real-time deployment within routine clinical workflows.

Disclosure of Interests. The authors have no competing interests to declare that are relevant to the content of this article.

References

1. Alzubaidi, M., Shah, U., Agus, M., Househ, M.: Fetsam: Advanced segmentation techniques for fetal head biometrics in ultrasound imagery. IEEE Open Journal of Engineering in Medicine and Biology **5**, 281–295 (2024). https://doi.org/10.1109/OJEMB.2024.3382487
2. Avisdris, N., Joskowicz, L., Dromey, B., David, A.L., Peebles, D.M., Stoyanov, D., Ben Bashat, D., Bano, S.: Biometrynet: Landmark-based fetal biometry estimation from standard ultrasound planes. In: Wang, L., Dou, Q., Fletcher, P.T., Speidel, S., Li, S. (eds.) Medical Image Computing and Computer Assisted Intervention – MICCAI 2022. pp. 279–289. Springer Nature Switzerland, Cham (2022)
3. Bach, S.H., Broecheler, M., Huang, B., Getoor, L.: Hinge-loss markov random fields and probabilistic soft logic. J. Mach. Learn. Res. **18**(1), 3846–3912 (Jan 2017)
4. Baumgartner, C.F., Kamnitsas, K., Matthew, J., Fletcher, T.P., Smith, S., Koch, L.M., Kainz, B., Rueckert, D.: Sononet: Real-time detection and localisation of fetal standard scan planes in freehand ultrasound. IEEE Transactions on Medical Imaging **36**(11), 2204–2215 (November 2017). https://doi.org/10.1109/TMI.2017.2712367
5. Chougule, A., Roy, P., Wagh, M.G., Goyal, D.: Artificial intelligence-based estimation of fetal head circumference with biparietal and occipitofrontal diameters using two-dimensional ultrasound images. Journal of Engineering and Science in Medical Diagnostics and Therapy **8**(2), 021103 (08 2024). https://doi.org/10.1115/1.4065799, https://doi.org/10.1115/1.4065799
6. Dosovitskiy, A., Beyer, L., Kolesnikov, A., Weissenborn, D., Zhai, X., Unterthiner, T., Dehghani, M., Minderer, M., Heigold, G., Gelly, S., Uszkoreit, J., Houlsby, N.: An image is worth 16x16 words: Transformers for image recognition at scale. In: International Conference on Learning Representations (2021), https://openreview.net/forum?id=YicbFdNTTy
7. Gao, P., Geng, S., Zhang, R., Ma, T., Fang, R., Zhang, Y., Li, H., Qiao, Y.: Clip-adapter: Better vision-language models with feature adapters. International

Journal of Computer Vision **132**(2), 581–595 (2024). https://doi.org/10.1007/s11263-023-01891-x, https://doi.org/10.1007/s11263-023-01891-x
8. Kompella, G., Antico, M., Sasazawa, F., Jeevakala, S., Ram, K., Fontanarosa, D., Pandey, A.K., Sivaprakasam, M.: Segmentation of femoral cartilage from knee ultrasound images using mask r-cnn. In: 2019 41st Annual International Conference of the IEEE Engineering in Medicine and Biology Society (EMBC). pp. 966–969 (2019). https://doi.org/10.1109/EMBC.2019.8857645
9. Krishna, T.B., Poreddy, A.K.R., Sindhu, K.G., Kokil, P.: Automated maternal fetal ultrasound image identification using a hybrid vision transformer model. In: Antonacopoulos, A., Chaudhuri, S., Chellappa, R., Liu, C.L., Bhattacharya, S., Pal, U. (eds.) Pattern Recognition. pp. 253–269. Springer Nature Switzerland, Cham (2025)
10. Loshchilov, I., Hutter, F.: Decoupled weight decay regularization. In: International Conference on Learning Representations (ICLR) (2019), https://arxiv.org/abs/1711.05101
11. Ma, J., He, Y., Li, F., Han, L., You, C., Wang, B.: Segment anything in medical images. Nature Communications **15**(1), 654 (2024). https://doi.org/10.1038/s41467-024-44824-z, https://doi.org/10.1038/s41467-024-44824-z
12. Ma, L., Li, K., Xiao, Z., Tan, G., Wen, H., Li, S.: Structure-aware fine-grained instance segmentation for fetal brain ultrasound images. Neurocomputing p. 133093 (2026). https://doi.org/https://doi.org/10.1016/j.neucom.2026.133093, https://www.sciencedirect.com/science/article/pii/S092523122600490X
13. Murugesan, B., Vijaya Raghavan, S., Sarveswaran, K., Ram, K., Sivaprakasam, M.: Recon-glgan: a global-local context based generative adversarial network for mri reconstruction. In: International workshop on machine learning for medical image reconstruction. pp. 3–15. Springer (2019)
14. Salomon, L.J., Alfirevic, Z., Berghella, V., Bilardo, C.M., Chalouhi, G.E., Da Silva Costa, F., Hernandez-Andrade, E., Malinger, G., Munoz, H., Paladini, D., Prefumo, F., Sotiriadis, A., Toi, A., Lee, W.: Isuog practice guidelines (updated): performance of the routine mid-trimester fetal ultrasound scan. Ultrasound in Obstetrics & Gynecology **59**(6), 840–856 (2022). https://doi.org/https://doi.org/10.1002/uog.24888, https://obgyn.onlinelibrary.wiley.com/doi/abs/10.1002/uog.24888
15. Tehsin, S., Alshaya, H., Bouchelligua, W., Nasir, I.M.: Hybrid state–space and vision transformer framework for fetal ultrasound plane classification in prenatal diagnostics. Diagnostics **15**(22) (2025). https://doi.org/10.3390/diagnostics15222879, https://www.mdpi.com/2075-4418/15/22/2879
16. Wang, Q., Zhao, D., Ma, H., Liu, B.: Fb-zwunet: A deep learning network for corpus callosum segmentation in fetal brain ultrasound images for prenatal diagnostics. Biomedical Signal Processing and Control **104**, 107499 (2025). https://doi.org/https://doi.org/10.1016/j.bspc.2025.107499, https://www.sciencedirect.com/science/article/pii/S1746809425000102
17. Yang, C., Zhang, C., Yang, X., Li, Y.: Performance study of cbam attention mechanism in convolutional neural networks at different depths. In: 2023 IEEE 18th Conference on Industrial Electronics and Applications (ICIEA). pp. 1373–1377 (2023). https://doi.org/10.1109/ICIEA58696.2023.10241832
18. Yousefpour Shahrivar, R., Karami, F., Karami, E.: Enhancing fetal anomaly detection in ultrasonography images: A review of machine learning-based approaches. Biomimetics **8**(7) (2023). https://doi.org/10.3390/biomimetics8070519, https://www.mdpi.com/2313-7673/8/7/519

19. Zhao, L., Li, K., Pu, B., Chen, J., Li, S., Liao, X.: An ultrasound standard plane detection model of fetal head based on multi-task learning and hybrid knowledge graph. Future Generation Computer Systems **135**, 234–243 (2022). https://doi.org/https://doi.org/10.1016/j.future.2022.04.011, https://www.sciencedirect.com/science/article/pii/S0167739X22001340